8th US National Combustion Meeting
Organized by the Western States Section of the Combustion Institute
and hosted by the University of Utah
May 19-22, 2013.

Direct Numerical Simulations of Diffusion Flame Extinction at Different Pressures

Vivien R. Lecoustre[1] *Paul G. Arias*[2] *Somesh Roy*[3] *Z. Luo*[4]
Dan C. Haworth[3] *Hong G. Im*[2,5] *Tianfeng F. Lu*[4] *Arnaud Trouvé*[1]

[1]*University of Maryland, College Park, MD 20742*

[2]*University of Michigan, Ann Arbor, MI 48109*

[3]*Pennsylvania State University, University Park, PA 16802*

[4]*University of Connecticut, Storrs, CT 06269*

[5]*King Abdullah University of Science and Technology, Thuwal 23955, Saudi Arabia*

Direct numerical simulations (DNS) of ethylene/air diffusion flames in decaying two-dimensional turbulence were performed to investigate flame extinction characteristics at different pressures. A Damköhler number based flame extinction criterion as provided by classical large activation energy asymptotic (AEA) theory is also assessed for its validity in predicting flame extinction induced by strain and heat losses. The DNS code, S3D, solves compressible flow conservation equations using a high order finite difference and explicit time integration schemes. The ethylene/air flame behavior is described by employing a reduced mechanism that accurately describes up to C_4 chemistry by the directed relation graph (DRG) method along with stiffness removal. The model configuration is an ethylene fuel strip embedded in ambient air on both sides, which is superimposed by a prescribed decaying turbulent flow field. Due to the high spatial and temporal stiffness associated with the detailed chemistry, a spatial resolution of 8 μm was used, and the time resolution was varied from 5 to 10 ns. A total physical time of 1 ms was computed in order to observe the temporal evolution of diffusion flame extinction events. The emphasis of this study is on the several flame extinction events observed in the simulations. The effect of pressure on extinction is studied by considering three different pressures: 0.1, 1.0, and 10 atm. To isolate the pressure effects on the turbulence and those on the chemistry, contrived physical parameters were considered by artificially changing the gas transport properties in relation with the pressure change. This methodology allows a consideration of identical turbulent flow fields at different pressure conditions. An extinction criterion based on the local Damköhler number is tested for its validity in predicting various flame extinction events encountered. Results show that, despite the relative simplicity of the AEA flame extinction criterion, it can accurately predict the flame extinction conditions. In particular, radical concentrations near the stoichiometric mixture fraction isocontour follow similar trends at extinction for all pressure conditions considered. A more rigorous mathematical approach based on the chemical explosive mode analysis (CEMA) was used in comparison with the AEA-based diagnostic. It is found that the AEA flame extinction criterion provides identifications of extinction events that are consistent with those provided by CEMA. This study supports the validity of a simple Damköhler number based criterion to predict flame extinction in engineering-level CFD models.

1 Introduction

Flame extinction in non-premixed flames is a pivotal subject of research in combustion science and has important ramifications for engineering applications; whether the interest lies in power

generation applications or in fire safety. The seminal work of Linãn [1] has provided the mathematical foundations for the study of non-premixed flame extinction in counterflow flame configuration. Several authors have then succeeded and extended the extinction analysis to different non-premixed flame configurations [2–4], with various level of heat losses [3, 5], and in turbulent regime [6]. Further references and descriptions are provided in the reviews by Williams [7, 8]. These studies have shown that extinction can be explained by the Damköhler number, which is the ratio of a characteristic mixing time over a characteristic chemical time.

Direct Numerical Simulations provide a valuable platform for the understanding of the physics of flames. Several past DNS works have focused on non-premixed flame extinction in various environments [9–12]. Past work from this group was dedicated to applying a flame extinction criterion to local flame quenching by water-spray [9], flame extinction due to high soot load [11], or due to flame interactions with a cold wall [12]. Narayanan *et al.*, [13], have derived a similar Damköhler number based extinction criterion using large activation energy asymptotic analysis (AEA) and studied the extinction limits of laminar counterflow diffusion flames as a function of flame stretch and radiant losses due to soot and gas-phase species. A parametrization of this criterion was performed in subsequent work for conditions with various levels of radiation losses, strain, and reactant vitiations [14]. These studies have lead to a critical Damköhler number based flame extinction.

The objectives of this present work are to use DNS to simulate non-premixed flame extinction due to sustained high mixing levels at different pressures, and to study the applicability of the AEA-based Damköhler extinction criterion to these flames. We will show how the pressure effects on turbulence can be decoupled from the pressure effects on chemistry using a modified flow viscosity so that the conclusions are independent of the turbulence. Some aspects of the flame structure are then related to the extinction criterion. Finally, a brief comparison of extinction diagnostic provided by the Chemical Explosive Mode Analysis (CEMA), Ref. [15], with the AEA derived criterion is performed.

2 Numerical Method

2.1 Flow Solver

The DNS solver, named S3D, employs an explicit 4^{th} order Runge-Kutta (ERK) time integration [16] and an 8^{th} order central finite-differencing schemes [17] for accurate integration of the compressible form of the Navier-Stokes equations. Boundary conditions are treated using Navier-Stokes Characteristic Boundary Conditions (NSCBCs) described in Ref. [18]. Further information and discussion on the governing equations and the boundary conditions can be found in Refs. [9, 10, 12, 19] and references therein.

Transport properties are evaluated using a mixture averaged model, calculated from the transport libraries provided by wrappers to the CHEMKIN package [20]. The code is highly modular, incorporating advanced multi-physics such as radiation [12], soot models [11], water droplet dynamic [9], that have previously been used.

2.2 Reduced Chemical Model

The detailed mechanism used was first proposed by Appel *et al.* [21]. It is a C_2H_4-air reaction model that includes 101 species and 542 elementary reactions. This model includes growth of PAH beyond benzene through the HACA mechanism up to pyrene ($C_{16}H_{10}$). The mechanism is large in size and is also chemically stiff. The integrated approach in Ref. [22] was employed in the present study to obtain a non-stiff reduced mechanism suitable for DNS. First, the method of DRG-aided sensitivity analysis was applied to eliminate unimportant species and reactions from the detailed mechanism. A skeletal mechanism with 67 species and 342 reactions was obtained by limiting the worst-case error to be less than 20% in ignition delays, extinction times in perfectly stirred reactors (PSR), pyrene concentrations in PSR, and laminar premixed flame speeds. The reduction covered the parameter range of pressure 0.1 to 10 atm, equivalence ratio ϕ = 0.5 to 2.0, and initial temperature above 1000 K for ignition. Second, linearized quasi steady state approximations (LQSSA) were applied to seven species, namely CH, CH_2, CH_2·, CH_2OH, CH_3O, C_2H, $n-C_6H_5$, which were identified to be in quasi steady state (QSS) for all the investigated conditions using a criterion based on CSP [23]. A 56 step reduced mechanism was hereby obtained with the QSS species concentrations solved analytically [24]. In the end, dynamically stiffness removal [22] was applied on the mechanism to eliminate chemical time scales shorter than 10 ns. This limiting time step value is typically of the order of the limit imposed by the CFL number in our compressible flow simulations, where a typical time step of value Δt = 7 ns is adopted.

2.3 DNS configuration

The present aim of this work is to numerically investigate the effects of flame stretching leading to extinction in different pressure configurations and to validate the applicability of a Damköhler number based extinction criterion for diffusion flames. Since the dynamics of the turbulence are not of interest but only their stirring and flame wrinkling effects, a 2D configuration is adopted. This offers a more convenient framework for the present investigation. The adopted configuration is that of a temporally evolving jet diffusion flame initially immersed in a decaying turbulent field. The flame initial condition corresponds to that of a 1D laminar diffusion flame with a moderate scalar dissipation rate, $\chi_{st} = 2\alpha_{mixture}\|\nabla Z\|^2_{Z=Z_{st}} \simeq 7\ s^{-1}$. Figure 1 plots the initial mixture fraction profile along the $\vec{X}$ direction.

Temperature and species fields were initialized using a flamelet solution generated from a counterflow configuration with a matching value of χ_{st}. The flamelet was generated with OPPDIF using the same chemical model. The initial flame profile was immersed into an initial isotropic, homogeneous 2-D turbulent flow field generated with the Passot-Pouquet energy spectrum [25].

The RMS fluctuating velocity was set to 8 m/s while the mean velocity was set to 0 m/s. The length of the most energetic scale was set to 1 mm. The integral length scale, $L_{i,ii}$, and the Kolmogorov length scale were equal to 0.338 mm and 14 μm, respectively. The eddy turn-over time is τ = 0.013 ms.

The initial turbulent Reynolds number, $\Re_T$, was equal to 173. The same turbulent parameters were used for all the cases. In order to minimize the interactions between the turbulent flow and the boundaries, the turbulent field was spatially filtered within 5 mm near each $\vec{X}$ boundary. This

avoided any artificial pressure disturbances that happen when a vortex leaves the computational domain.

The rectangular, two-dimensional computational domain was 2.5 cm long and 1.4 cm wide. A uniform, Cartesian mesh grid was used with a mesh spacing of 8 μm. This value represents the largest mesh spacing required to solve accurately the reacting layer near strain-induced extinction for all the pressures considered in the present study. This value was determined by OPPDIF. The total number of grid point was 5,250,000. The workload was shared by 2100 CPUs. The time step was chosen depending on the pressure. At low pressure, the time step was set to 10 ns; at atmospheric pressure, it was set to 7.2 ns; and at high pressure, the time step was set to 5 ns. Each simulation represents about 200,000 CPU hours.

2.4 Modified Diffusive Properties Approach

In order to study the influence of the pressure on the flame, the same configuration was considered at 0.1, 1, and 10 atm. As the interest of this work is the chemical kinetic response of the flame under various local stretch conditions, it is desired to keep the turbulence characteristics independent of the pressure applied to the system. Turbulent flow characteristics at 1 atm were established as reference.

The Kolmogorov theory states that the dynamic of the turbulence is controlled by the large scales and by the inherent flow physical properties corresponding to dissipative effects, namely the kinematic viscosity ν. If the large scale generating conditions are kept identical independently of the pressure applied to the system, then in order to obtain a similar turbulent behavior, ν must be kept independent of the pressure. Since $\nu = \dfrac{\mu}{\rho}$, where ρ is the density of the fluid, consideration of the ideal gas law gives:

$$\nu \sim \frac{\mu}{P}. \tag{1}$$

In order to keep the kinematic viscosity independent of the pressure, the dynamic viscosity of the fluid has to be rendered dependent of the pressure with the relation:

$$\mu = \mu_0 P. \tag{2}$$

This allows identical turbulent behavior when the same initial conditions are applied to the system regardless of the pressure considered.

In order to keep the relative strength of the heat dissipative effects and the relative species transport effects consistent with the reference conditions at 1 atm, the mixture conductivity and the species diffusivity were adjusted so that the Prandlt, Lewis, and Schmidt numbers were unaffected by the modification of the dynamic viscosity. In this framework, the levels of diffusive fluxes of species, momentum, and heat remain comparable in all cases, regardless of the pressure applied. This provides a unique and consistent configuration for which only the chemical source terms were affected by pressure. The transport properties remained similar to those at the pressure of reference and the hydrodynamic effects were kept constant, at least at first order.

3 Results

3.1 Validation of Modified Viscosity

The present modified viscosity approach has been validated with an *a priori* and an *a posteriori* analysis by comparing qualitatively the flame evolution and quantitatively by comparing the statistical distribution of the scalar dissipation rate simulated with a simplified single step chemistry model, and during the execution of the simulations with the reduced detailed chemistry. Details about the single chemistry model can be found in Wang *et al.* [12].

Figure 2 plots the non-normalized conditioned scalar dissipation rate χ at $Z = Z_{st}$ at 0.5 ms for a simulation realized at atmospheric pressure and for another realized at 10 atm, with the approach presented in Section 2.4. The distributions are both qualitatively and quantitatively comparable; the mean, maximum, minimum values, and standard deviation of the scalar dissipation rate are similar at 1 and 10 atm. Small differences exist due to differences in the mesh used - the 10 atm case has a more refined grid - and to the slightly higher temperatures predicted at 10 atm.

3.2 Flame Evolution

Figures 3 and 4 plot the instantaneous temperature fields at various times of the simulations, from initialization to the end of the simulations, set at 1 ms. The pressure in Fig. 3 is 1 atm, whereas it is 10 atm in Fig. 4. The qualitative temporal evolution is similar for both pressures as a result of the modified viscosity approach. Interactions between the flame and the flow field can be readily observed. The flame is not uniformly affected by the turbulence; local parts of the flame are being stretched with more intensity than others. An extinction event can be seen in Fig. 3, happening from 0.3 ms to 0.55 ms, in the lower left quadrant of the field, near x = -0.4 cm and y = 0.5 cm. This strain induced quenching reignites afterward. While similar stretching happens at 10 atm, Fig. 4 does not show any discontinuity in the temperature field at the time considered above. This reflects the absence of extinction at higher pressure. More extinction events were predicted at 0.1 atm than at 1.0 atm. Using the AEA Damköhler number based criterion, about 5 extinction events were predicted at 0.1 atm, while only 2 were predicted at 1 atm, and none at 10 atm.

While the effects of pressure on the turbulence dynamics have been mitigated by varying the flow viscosity, pressure effects on the chemistry are still present, as illustrated in Fig. 5 which plots the temporal evolution of the domain integrated heat release rate for the three pressures considered. A factor of about 10 exists between the three curves and as expected, the heat release rate increases with pressure.

The effects of flow turbulence on the flames are characterized by the value of the scalar dissipation rate at the location of stoichiometry, χ_{st}. Figure 6 plots the conditional mean of the scalar dissipation rate at locations of stoichiometry and its standard deviation for the three pressures. All have similar evolution, and they only differ in values. Starting from an initial value of about 7 s^{-1}, the mean χ_{st} quickly plateaus to values near 15 s^{-1}, and remains nearly constant for the first 0.2 ms of the simulation before undergoing a rapid increase, and peaking slightly before 0.4 ms. Then a less pronounced steady decline is observed. The standard deviation of χ_{st} follows the same similar trend, peaking at the same time as the peak of mean χ_{st}. Note that the predicted standard deviation

of χ_{st} is generally greater than the mean χ_{st}. This indicates an important spreading of the local stoichiometric scalar dissipation rates, and the potential for extinction events. Note that the shape of Fig. 6 is dependent on the chosen turbulence initial conditions.

4 Discussion

4.1 Flame Extinction

It is well-known that large values of χ_{st} can lead to aerodynamic quenching [1, 26]. In previous work done by this group, a flame weakness factor criterion has been introduced to describe extinction. It is expressed here as a scaled Damköhler number:

$$Da = \frac{\chi_{st,ext}}{\chi_{st}} \exp\left(T_a \left(\frac{1}{T_{st,ext}} - \frac{1}{T_{st}}\right)\right), \tag{3}$$

where the subscript st denotes conditions at extinction and T_a is an effective activation temperature. Values of $\chi_{st,ext}$ and $T_{st,ext}$ were obtained for the three pressures considered by simulating counterflow diffusion flame extinction using OPPDIF [27] with the same chemical model as used the DNS and the same modified viscosity approach.

P (atm)	$\chi_{st,ext}$ (s^{-1})	$T_{st,ext}$ (K)	T_a (K)
0.1	12.5	1475	12292
1	116	1745	18692
10	1026	1939	19250

Table 1: Stoichiometric scalar dissipation rates and temperatures predicted at extinction conditions for the pressures considered. The corresponding activation energy are also tabulated; they have been calculated from simulated premixed flame laminar flame speed at the pressures considered with the modified viscosity approach.

These values are given in Table 1. Values of the activation energy are also reported in this table and they are found to vary with the pressure considered. The aforementioned criterion has been applied to laminar counterflow diffusion flames undergoing aerodynamic quenching and radiative extinction in Ref. [14]. It has been shown that its value at extinction, with appropriate scaling independent of the extinction mechanism, remains close to unity.

Values of Da has been calculated using Eq. 3 for the three pressure cases. Figure 7 plots the spatial variation of Da along the isocontour of stoichiometric mixture fraction for some selected times at 1 atm. Large values of Da correspond to steady burning flames, while low values of Da correspond to conditions near extinction. Extinction locations are defined as locations where $Da < 1$. This figure shows the dynamics of an extinction event that starts at 0.25 ms and lasts until 0.7 ms. This event is characterized by the small values of Da at 0.305 ms and 0.405 ms. It occurs due to the high strain of the flame generated by intense mixing processes at this location. This extinction event is shown in Fig.3.

In order to further push the analysis associated with flame extinction, some aspects of the flame structure have been analyzed near the location of the stoichiometric isocontour. Since the flame chemistry is finite, the reaction zone has a thickness that spans in the direction normal to the stoichiometric isocontour. The vector $\vec{n} = \nabla Z|_{st}$ defines a local vector normal to the stoichiometric isocontour. For each location along it, the maximum value of some selected radicals has been sought along the normal direction n over some distance l. The researched location encompassed the stoichiometric line; maximum values were sought on both fuel and oxidizer sides. Figure 8 illustrates this concept. The length of investigation was set to 1 mm. This distance was shorten in case of non-monotonous variations of the mixture fraction to avoid merging effects due to the proximity of other flame fronts.

Maximum values of radicals were then obtained for each corresponding location on the isocontour. Each of the local extinction events has been identified and their temporal evolution monitored. On each segment of the stoichiometric line corresponding to an extinction event, the maximum value of selected radicals associated with the lowest Damköhler number has been extracted. Figure 9 plots the variations of the maximum mass fraction of the hydroxyl radical OH with the local Da at locations corresponding to local extinction events. The radical OH has been selected since it is involved in one of the most important reactions in a combustion process [26], the chain branching reaction:

$$\mathrm{H} + \mathrm{O}_2 \rightleftharpoons \mathrm{O} + \mathrm{OH} \tag{4}$$

Figure 9 plots values of peak OH for extinction events only; they correspond to a decreasing Da with time. Reignition events were not considered since they are not strictly in the diffusion flame mode and therefore the aforementioned criterion cannot be applied.

Figure 9 shows that regardless of the pressure, a common trend is observed in the evolution of the maximum value of Y_{OH} with Da. Three regimes exist. The first one corresponds to steady burning conditions observed at large values of Da, typically $Da > 20$. In this region, a change in Da will not affect the values of Y_{OH}. A transition region exists for Da between 20 to 0.05. In this region, a decrease of Da leads to a dramatic decrease of OH mass fraction. This is a sign of a strong weakening of the flame. For values of Da less than 0.05, OH vanishes, which indicates extinction. This behavior is observed independently of the pressure considered. These results show that the AEA Damköhler number criterion, which has been derived from asymptotic analysis under the assumption of single step chemistry can be effectively applied to detailed chemistry applications.

4.2 CEMA Analysis

A more sophisticated extinction diagnostic is provided by the Chemical Explosive Mode Analysis (CEMA) [15]. It provides a straightforward tool to analyze the complex chemical mechanisms involved in combustion. It has been applied to turbulent lifted hydrogen jet flames in hot coflow [23] and in lifted ethylene jet flames [15]. CEMA is based on the analysis of the eigenvalues of the Jacobian matrix of the chemical source terms. Eigenvalues have units of inverse chemical time scales. In particular, the sign of the eigenvalue is important and it determines the stability of the chemical source term. To simplify, a negative eigenvalue corresponds to a stable equilibrium while a positive eigenvalue corresponds to an explosive mode, which is a feature of either ignition or extinction [15]. For spatially non-homogeneous mixtures, a CEMA based Damköhler number can

be defined as the ratio of the eigenvalue over the scalar dissipation rate.

CEMA was applied to the DNS for a pressure of 1 atm and a Damköhler number was computed. Figure 10 plots this resulting Damköhler number along the stoichiometric isocontour, at the same times as those plotted in Fig. 7. It allows a direct comparison of the two extinction diagnostics. Note that in Fig. 10, Da_{CEMA} is defined as:

$$Da_{CEMA} = \max(1, |\lambda_e/\chi_{st}|)^{-\mathrm{sign}(\lambda_e)} \tag{5}$$

where λ_e is an associated eigenvalue. With this definition, Da_{CEMA} is greater than unity for stable conditions, and lower than unity for unstable conditions, *i.e.* conditions with potential for extinction. It is seen in Fig. 10 that the locations of extinction events are the same as the locations of extinction events identified with the AEA-based Damköhler number. The value of Da computed by CEMA are less conservative than the ones computed from the AEA analysis. Indeed, at 0.65 ms CEMA shows that conditions for extinction are present in the location about 4 to 5 cm from the origin of the curvilinear coordinates, whereas the previous diagnostic only shows a weak sign of extinction at this location. While the flame at this location undergoes a significant level of strain, it does not extinguish. This whole analysis does not take into consideration the temporal aspect of the straining, which might explains this differences of behavior indicated by the two diagnostics.

5 Conclusion

Direct Numerical Simulations of a temporally evolving ethylene jet diffusion flame in air, initially immersed into a decaying turbulent field were performed for three different pressures: 0.1 atm, 1 atm, and 10 atm. In order to decouple the effects of pressure on the turbulence and on the chemistry, simulations were performed using a modified fluid dynamic viscosity and species diffusivity. Results show that within this framework, the turbulence dynamics are kept independent of the pressure. Several local extinction events were simulated and analyzed using a large activation energy asymptotic (AEA) analysis Damköhler-based criterion and another criterion provided by the more sophisticated Chemical Explosive Mode Analysis approach. It was shown that the AEA extinction criterion catches the evolution of the flame structure near extinction at all three pressures considered. It was found that the AEA extinction criterion provides identification of extinction events that are consistent with those identify by CEMA.

Acknowledgments

This work was sponsored by the National Science Foundation, PetaApps Program awarded to the multiple institutions, with grant numbers: OCI-0904660, OCI-0904480, OCI-0904649, OCI-0904771, OCI-0904818, OCI-0905008.

References

[1] Amable Liñán. *Acta Astronautica*, 1 (1974) 1007–1039.

[2] C.K. Law. *Combustion and Flame*, 24 (1975) 89–98.

[3] K Mills and M Matalon. *Combustion Science and Technology*, 129 (1997) 295–319.

[4] Buckmaster. Lecture 9 Spherical Diffusion Flames. In *"Lectures on mathematical combustion"*, Vol. 97, pages 97–107. 1983.

[5] Q. Wang and B.H. Chao. *Combustion and Flame*, 158 (2011) 1532–1541.

[6] N. Peters. *Combustion Science and Technology*, 30 (1983) 1–17.

[7] F.A. Williams. *Fire Safety Journal*, 3 (1981) 163–175.

[8] F A Williams. *Progress in Energy and Combustion Science*, 26 (2000) 657–682.

[9] P.G. Arias, H.G. Im, P. Narayanan, and A. Trouvé. *Proceedings of the Combustion Institute*, 33 (2011) 2591–2597.

[10] David O. Lignell, Jacqueline H. Chen, and Hans A. Schmutz. *Combustion and Flame*, 158 (2011) 949–963.

[11] Praveen Narayanan and Arnaud Trouvé. *Proceedings of the Combustion Institute*, 32 (2009) 1481–1489.

[12] Yi Wang and Arnaud Trouvé. *Combustion and Flame*, 144 (2006) 461–475.

[13] Praveen Narayanan, Howard R. Baum, and Arnaud Trouvé. *Proceedings of the Combustion Institute*, 33 (2011) 2539–2546.

[14] Vivien Lecoustre, Praveen Narayanan, Howard Baum, and Arnaud Trouve. *Fire Safety Science*, 10 (2011) 583–595.

[15] Zhaoyu Luo, Chun Sang Yoo, Edward S. Richardson, Jacqueline H. Chen, Chung K. Law, and Tianfeng Lu. *Combustion and Flame*, 159 (2012) 265–274.

[16] Christopher A. Kennedy, Mark H. Carpenter, and R.Michael Lewis. *Applied Numerical Mathematics*, 35 (2000) 177–219.

[17] Christopher A. Kennedy and Mark H. Carpenter. *Applied Numerical Mathematics*, 14 (1994) 397–433.

[18] M. Baum, T. Poinsot, and D. Thévenin. *Journal of Computational Physics*, 116 (1995) 247–261.

[19] C. S. Yoo, Y. Wang, A. Trouvé, and H. G. Im. *Combustion Theory and Modelling*, 9 (2005) 617–646.

[20] R.J. Kee, F.M. Rupley, E. Meeks, and J.A. Miller. Chemkin-iii: a fortran chemical kinetics package for the analysis of gas- phase chemical and plasma kinetics. Technical Report May, Sandia National Laboratories, 1996.

[21] Jörg Appel, Henning Bockhorn, and Michael Frenklach. *Combustion and Flame*, 121 (2000) 122–136.

[22] Tianfeng Lu and Chung K. Law. *Progress in Energy and Combustion Science*, 35 (2009) 192–215.

[23] T. F. Lu, C. S. Yoo, J. H. Chen, and C. K. Law. *Journal of Fluid Mechanics*, 652 (2010) 45–64.

[24] Tianfeng Lu and Chung K Law. *The journal of physical chemistry. A*, 110 (2006) 13202–8.

[25] T. Passot and A. Pouquet. *Journal of Fluid Mechanics*, 181 (1987) 441–466.

[26] Chung K. Law. *Combustion Physics*. Cambridge University Press, 2006.

[27] A.E. Lutz, R.J. Kee, J.F. Grcar, and F.M. Rupley. OPPDIF: a Fortran program for computing opposed- flow diffusion flames. Technical report, Sandia National Laboratories, Report SAND96-8243, 1996.

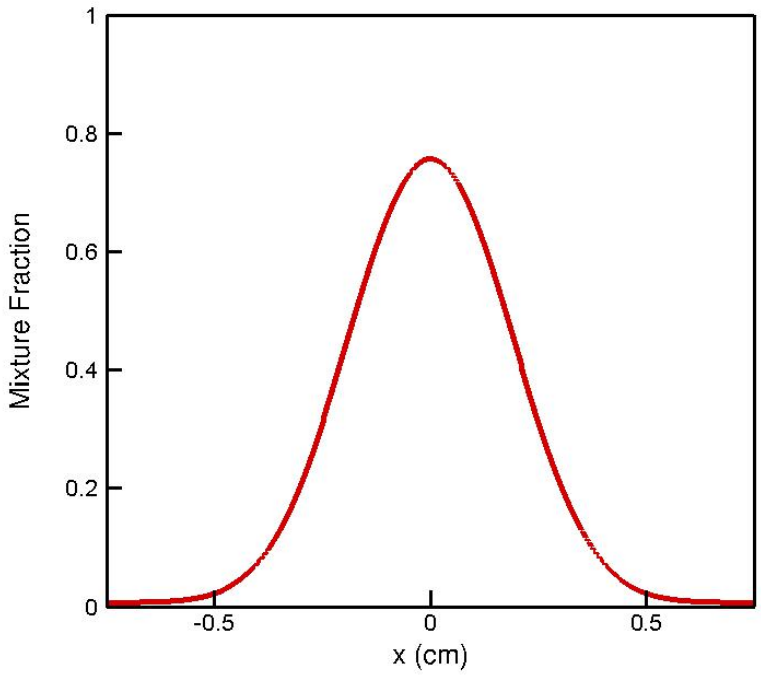

Figure 1: Initial mixture fraction profile along the x axis. The slope of this profile at location of stoichiometry is set such that χ_{st} = 7 s^{-1}.

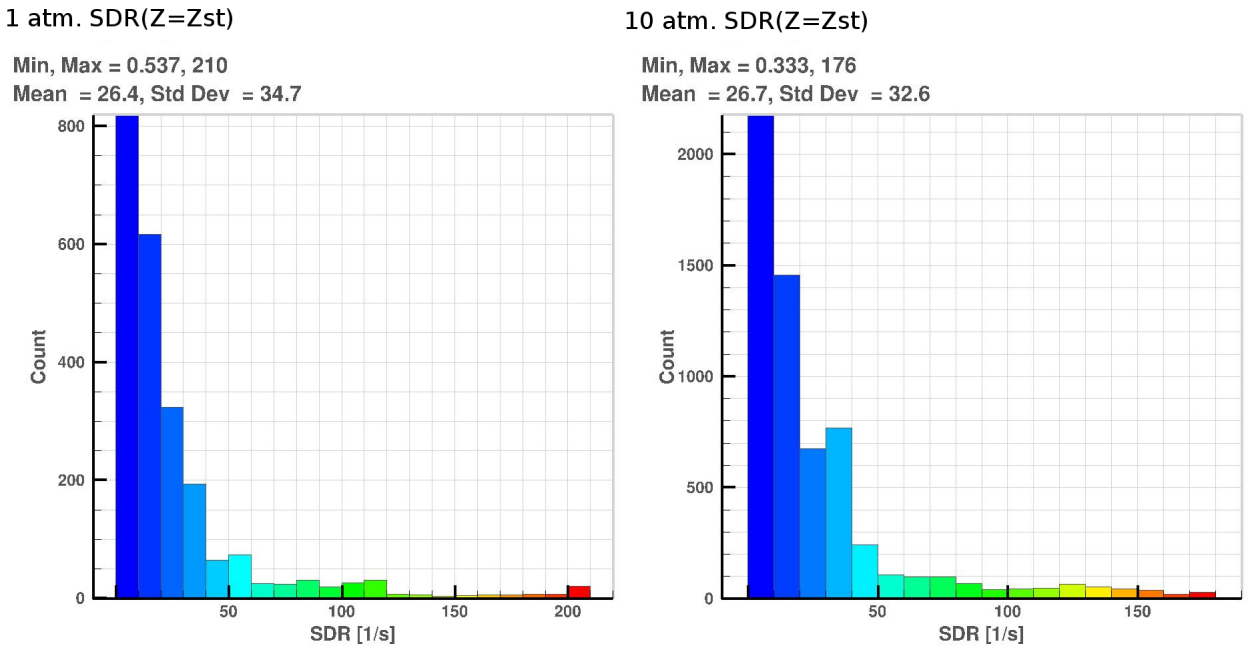

Figure 2: Non-normalized distributions of the stoichiometric scalar dissipation rate (SDR) predicted at 1 and 10 atm, 0.5 ms after initialization. A single step chemistry model was used for both pressures.

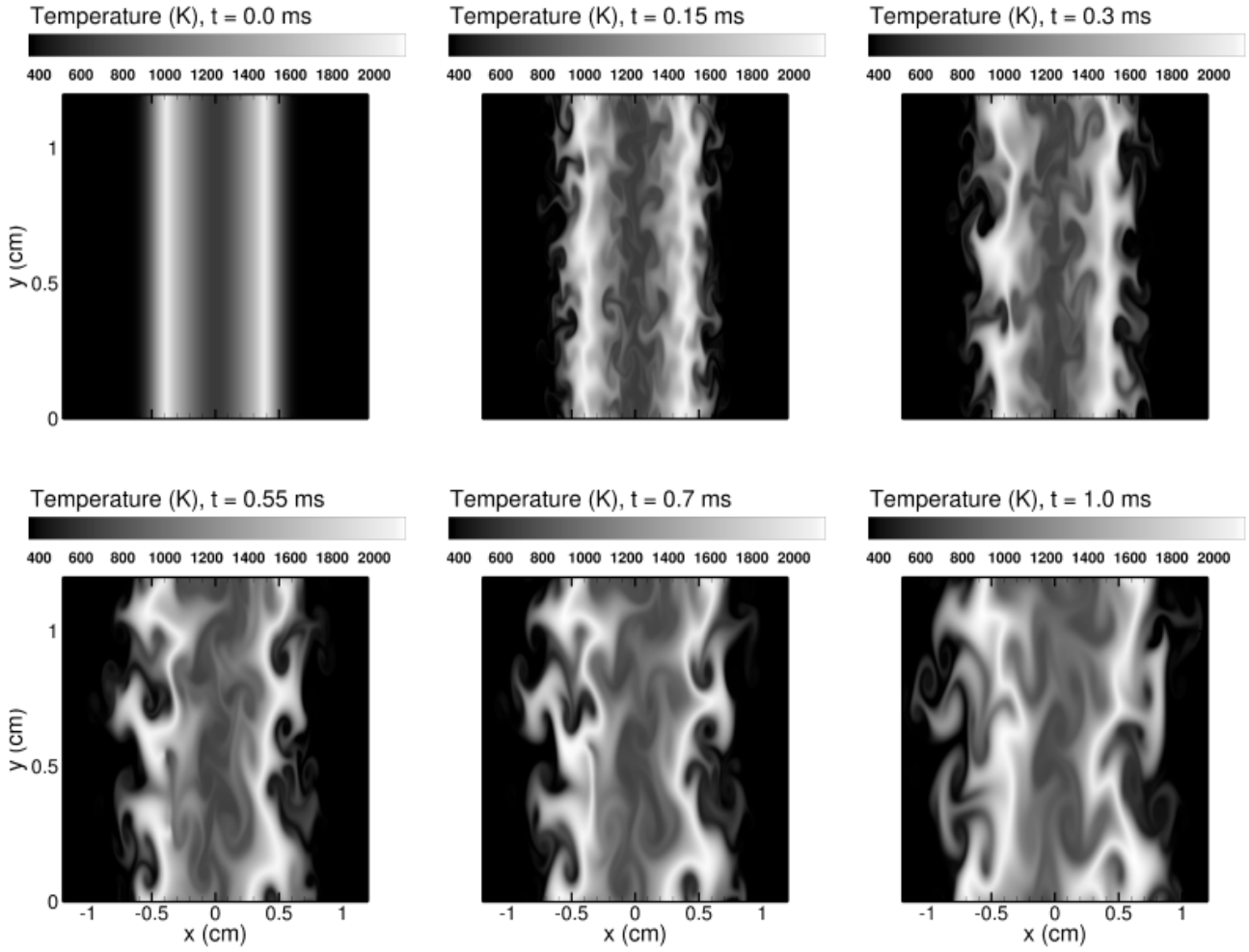

Figure 3: Instantaneous temperature fields predicted at 1 atm. The progressive wrinkling of the flame is observable as time elapses. Notice the extinction event at 0.55 ms translated by a region of lower temperatures in the vicinity of x = -0.4, y = 0.4 cm.

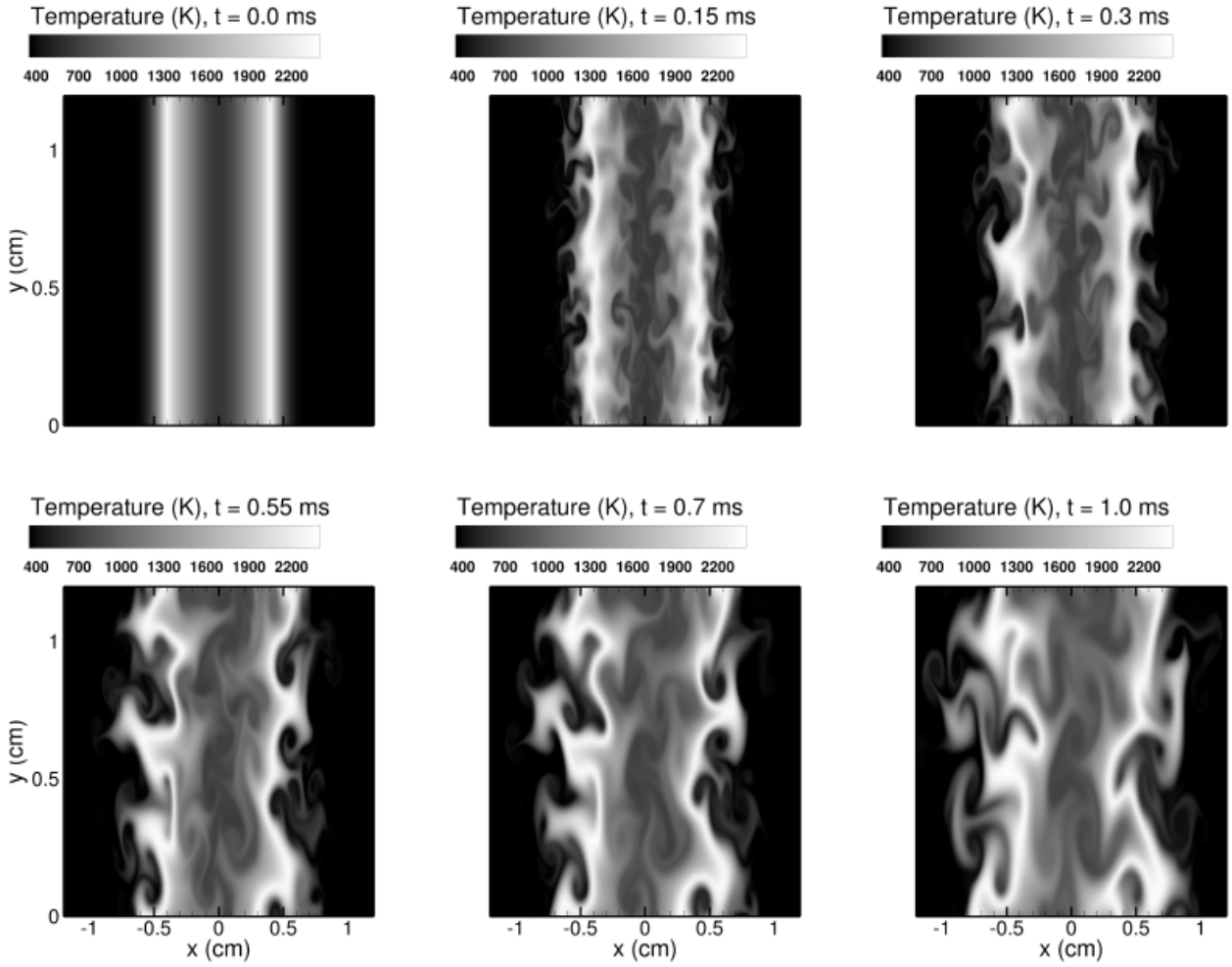

Figure 4: Instantaneous temperature fields predicted at 10 atm. The progressive wrinkling of the flame is observable as time elapses. Unlike the case at 1 atm, no extinction is predicted.

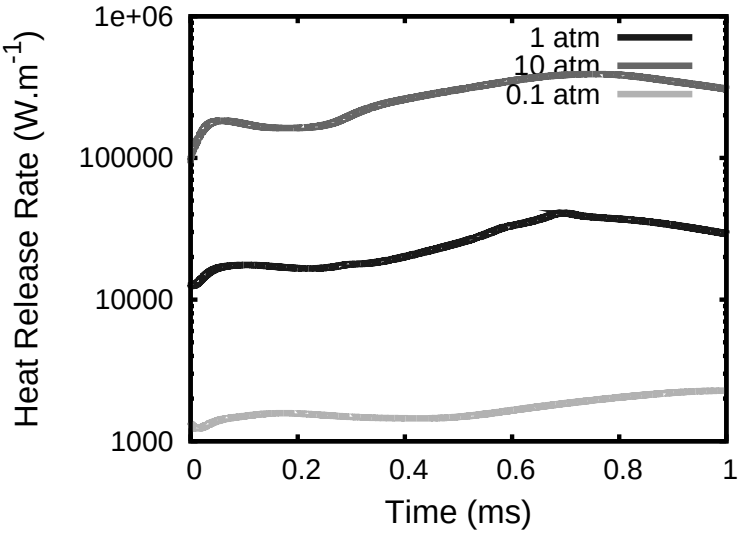

Figure 5: Temporal evolution of the domain integrated heat release rate for the three pressure cases considered.

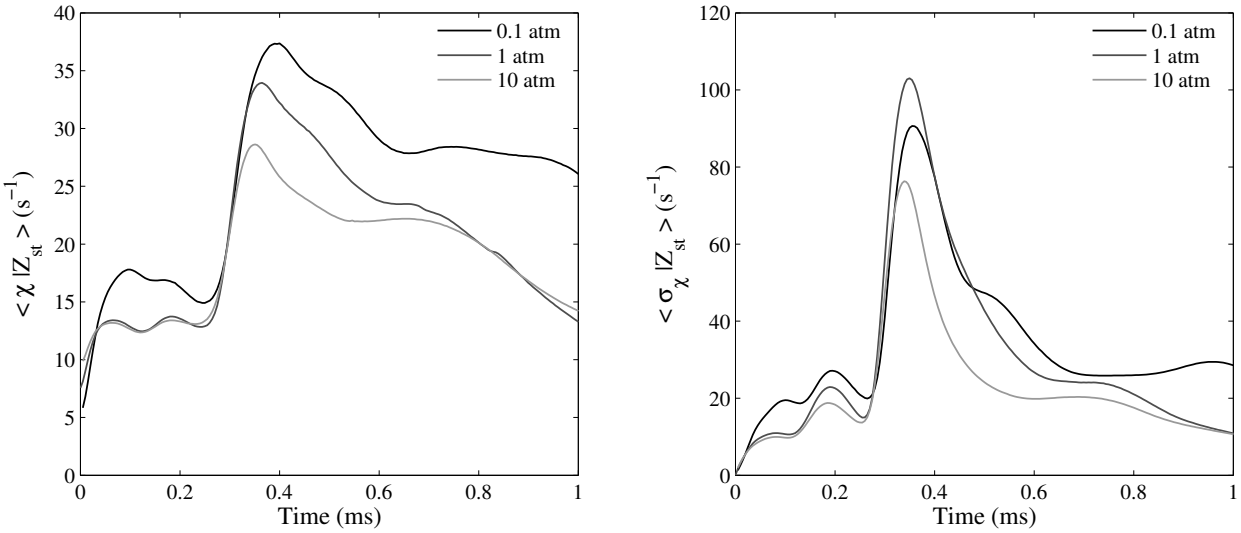

Figure 6: Temporal evolution of the conditional mean and standard deviation of the stoichiometric scalar dissipation rate at Z = Z_{st} for the three pressure cases considered: 0.1, 1, and 10 atm.

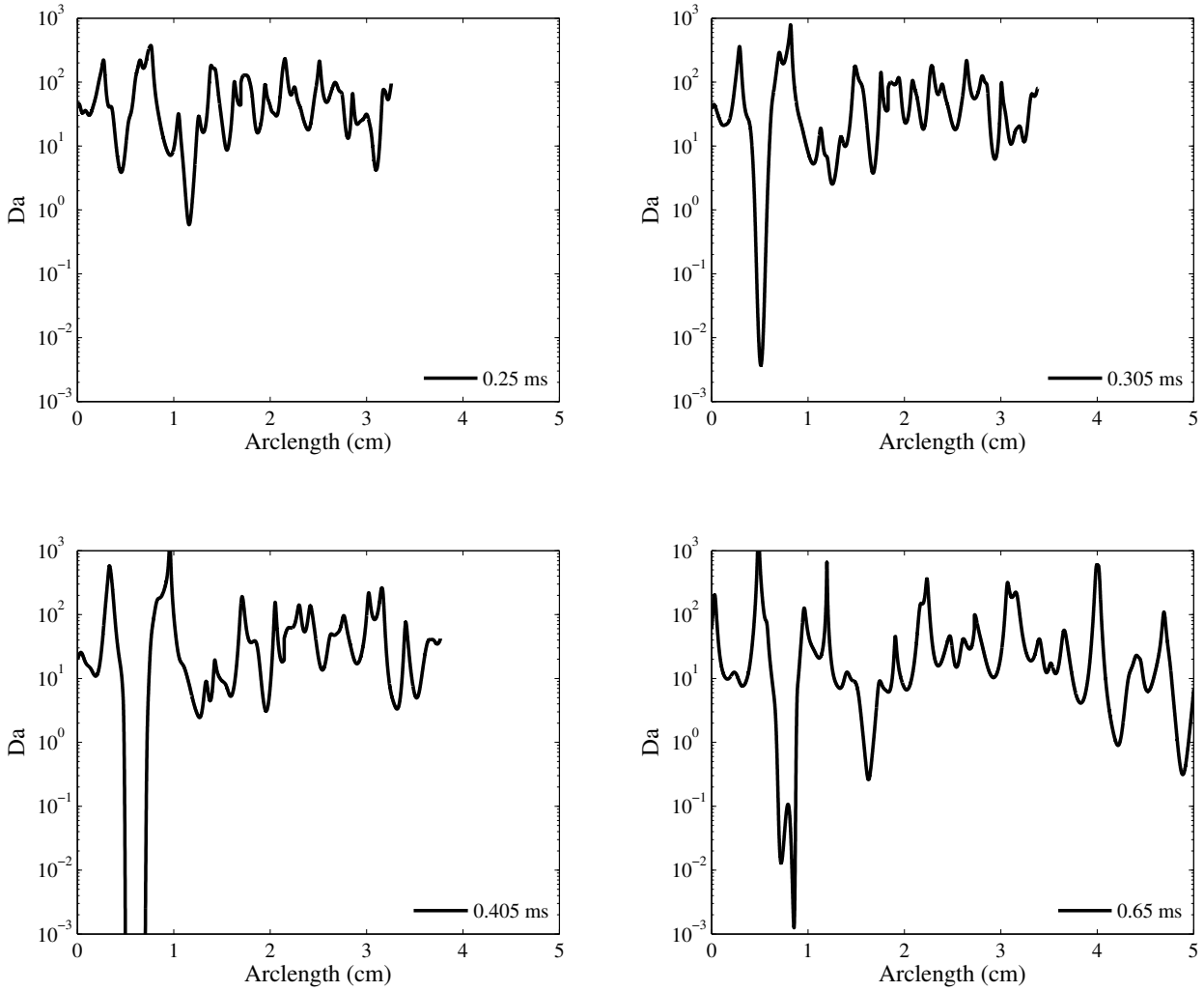

Figure 7: Spatial variation of the Damköhler number defined by Eq. 3 along the stoichiometric line. Extinction is defined for local conditions where $Da < 1$.

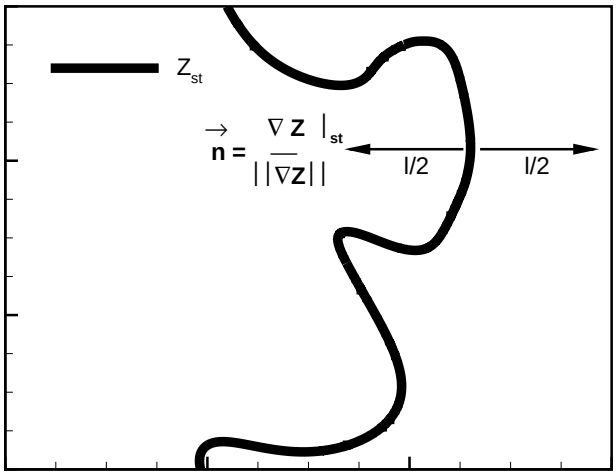

Figure 8: Maximum values of selected radicals are sought along the direction $\vec{n}$ normal to the line of stoichiometry. The distance of investigation is l and both fuel and oxidizer sides are considered.

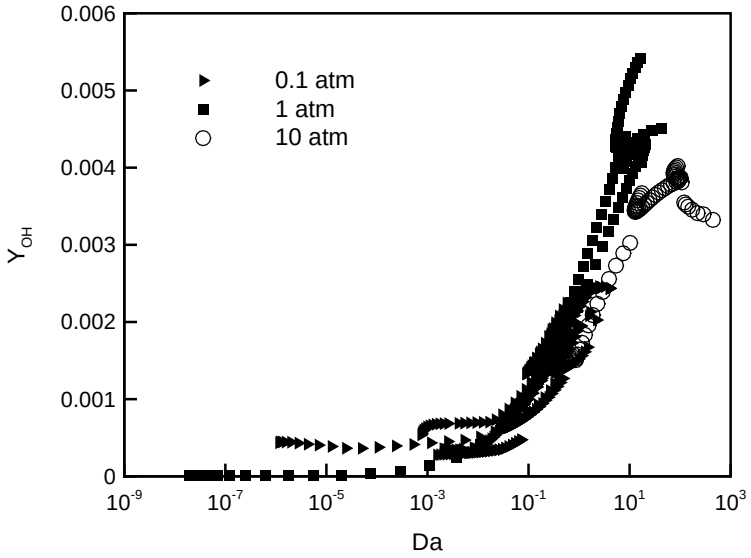

Figure 9: Peaks Y_{OH} variation for extinction events plotted against the associated Damköhler number. Three pressure cases are considered here.

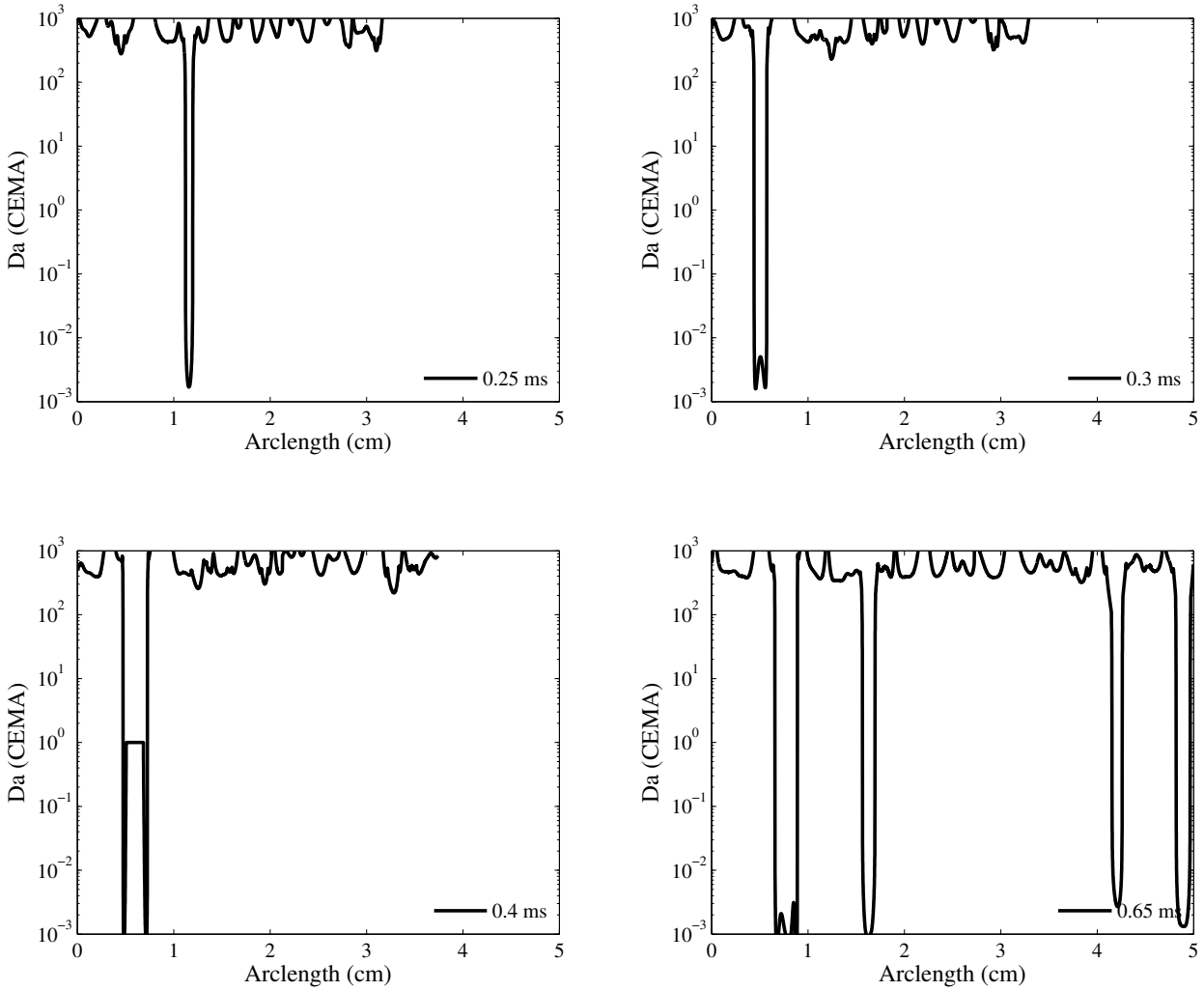

Figure 10: Spatial variations of the CEMA-based Damköhler number defined by Eq. 5 along the stoichiometric line. The trends are quantitatively similar to those predicted by the AEA-based Da criterion. Values of Da lower than unity correspond to unstable conditions, whereas values greater than unity correspond to stable conditions.